eprints@whiterose.ac.uk
https://eprints.whiterose.ac.uk/

Coupling Disturbance Compensated MIMO Control of Parallel Ankle Rehabilitation Robot Actuated by Pneumatic Muscles

Jie Zuo, Wei Meng, *Member, IEEE*, Quan Liu, Qingsong Ai, *Member, IEEE*, Sheng Q. Xie, *Senior Member, IEEE*

Abstract— **To solve the poor compliance and safety problems in current rehabilitation robots, a novel two-degrees-of-freedom (2-DOF) soft ankle rehabilitation robot driven by pneumatic muscles (PMs) is presented, taking advantages of the PM's inherent compliance and the parallel structure's high stiffness and payload capacity. However, the PM's nonlinear, time-varying and hysteresis characteristics, and the coupling interference from parallel structure, as well as the unpredicted disturbance caused by arbitrary human behavior all raise difficulties in achieving high-precision control of the robot. In this paper, a multi-input-multi-output disturbance compensated sliding mode controller (MIMO-DCSMC) is proposed to tackle these problems. The proposed control method can tackle the un-modeled uncertainties and the coupling interference existed in multiple PMs' synchronous movement, even with the subject's participation. Experiment results on a healthy subject confirmed that the PMs-actuated ankle rehabilitation robot controlled by the proposed MIMO-DCSMC is able to assist patients to perform high-accuracy rehabilitation tasks by tracking the desired trajectory in a compliant manner.**

I. INTRODUCTION

The recent meta-analysis reveals that there is 1.92 stroke patient per 100 person globally, and the total direct home and medical nursing costs are predicted to increasing from $396 billion to $918 billion, producing immense healthcare and economic burdens all over the world [1]. For instance, Chinese elderly population over 60 years old has reached 2.22 billion by the end of 2015, and stroke becomes the second leading cause of disability in elderly over 60 [1]. Most stroke patients are associated with ankle dysfunction, including lower limb muscle weakness, increased muscle tension, decreased control ability and sensory disturbance, resulting in abnormal gait, such as foot drop, pronation and unstable joint motion [2]. Therefore, it is urgent and important to recover the stroke patients' ankle movement ability and correct their hemiplegic gait. Relevant medical studies have shown that the aggressive rehabilitation program can enable 90% of stroke patients to regain their ability of walking and living independently [3]. A rehabilitation training program with 27 stroke patients for 12 weeks, and the results were associated with a significant 35% improvement in life heal evaluation compared with no training group [1]. However, due to the lack of rehabilitation treatment, the disability rate of stroke patients in is up to 75% . The global aging trend and the huge number of limb disability make the demand of clinical therapists and rehabilitation equipment, and thus the robot-assisted rehabilitation has been widely considered to be a promising non-therapist training approach for stroke patients [4].

However, most of the existing medical rehabilitation devices are actuated by rigid drives like motors, resulting in the insufficient flexibility and poor security in the process of rehabilitation training may even cause the secondary injury to the patients. Due to the motion regulation and physical characteristics similar to the bio-muscle, the pneumatic muscle (PM) becomes a promising choice, with the advantages of inherent compliance, large power-weight ratio and lightweight structure. Park *et al*. designed a wearable ankle rehabilitation robot, using the PMs to simulate the human ankle muscle-tenons-ligament model [5]. In this robot, each PM actuates the corresponding bio-muscle to assist the ankle joint perform dorsiflexion/plantarflexion and inversion-eversion movement. Likewise, Sawicki *et al.* also developed a series of soft ankle-foot orthosis based on the bionic joint drive structure [6, 7]. One of them is actuated by a single PM, which attached to the posterior to provide plantarflexion torque for the ankle joint [7]. However, the peak torque of this orthosis cannot cover the normal human ankle joint motion range, thus the later version was modified to be a parallel configuration driven by two PMs [6]. Though the above-mentioned ankle rehabilitation robots are able to assist the stroke patients to complete the basic training tasks to some extent, their loose and unfixed non-steel mechanism cannot provide sufficient support and assistance for stroke patients in their early rehabilitation stage. Parallel configuration possesses the characteristics of high stiffness and larger payload capacity. Moreover, it is feasible for the robots driven by the actuators in parallel configuration to provide multi-degrees-of freedom (DOF) motion assistance for a single joint, which is suitable for the ankle joint training. There have been some published researches on the parallel PMs-actuated mechanism; however, few of them are currently applied in the medical or rehabilitation field. Zhang *et al*. [8, 9] and Jamwal *et al*. [10] proposed two version of 3-DOF ankle rehabilitation robots driven by four PMs in parallel, which can help patients achieve 3-DOF movement in the ankle joint workspace. The former one is able to fix the patient's ankle joint on the robot gaiter, to avoid the influence of other joints' motion on the ankle joint [8]. However, both of these two robots' assistance torque for external/ internal rotation is too limited to meet the stroke's rehabilitation demands.

J. Zuo, W. Meng, Q. Liu, and Q. Ai are with the School of Information Engineering, Wuhan University of Technology, Wuhan 430070 China (e-mails: {zuojie weimeng, quanliu, qingsongai}@whut.edu.cn).

W. Meng is also with the School of Electronic and Electrical Engineering, University of Leeds, Leeds, LS2 9JT, UK (e-mail: w.meng@leeds.ac.uk).

S. Xie is with the School of Electronic and Electrical Engineering, University of Leeds, Leeds, LS2 9JT, UK (e-mail: s.q.xie@leeds.ac.uk).

PM's highly nonlinear, time varying characteristics and hysteresis phenomenon, as well as coupling interference existed in the parallel PMs-actuated configuration, make it hard to achieve high precision and robust control for PMs-actuated robots. PID control, fuzzy control and sliding mode control have been adopted in robot control field. However, it is challenging to utilize the former two control strategies in complexed and nonlinear PMs-driven robots, due to their linear control structure or complicated rules [11]. Ziegler-Nichols [12], inverse NARX fuzzy model [13], and knowledge-based adaptive compensator [14] were employed to enhance the performance of PID control and fuzzy control [15]. Compared with PID, sliding mode controller (SMC) can switch various control structures to adapt to the current state and is able to compensate PM's unpredicted disturbances and model uncertainties. However, due to the high switching frequency, the chattering problem always exists in SMC systems. To tackle the problem, Xing *et al*. introduced a nonlinear disturbance observer to reduce the SMC switch gains [16]. Likewise, a fuzzy logic controller was employed to approximate the switching control law [17, 18], which can compensate the nonlinear disturbance. For the ankle rehabilitation robot driven by PMs in parallel configuration, the control difficulties are not only related to PM's highly nonlinear and time-varying characteristics, but also caused by coupling interference during multiple PMs' synchronous movement. However, few studies considered the collaborative control between multiple PMs and how to eliminate the disturbance. Though Cao *et al*. proposed a multi-input multi-output controller, it is designed to control the pressure and compliance for a single PM at the same time, instead of synchronizing the movement of multiple PMs [19, 20].

In this paper, a novel soft parallel PMs-driven ankle rehabilitation robot is developed to provide sufficient assistance for the stroke's ankle rehabilitation. To compensate the PM's model uncertainty and coupling interference existed in multiple PMs' cooperation motion, we propose a modified multi-input-multi-output (MIMO) sliding mode controller with disturbance compensator (MIMO-DCSMC). The rest of paper is organized as follows. In Section II, the mechanism and models of the developed ankle rehabilitation robot are described. Section III proposes the modified disturbance compensated MIMO controller. Section IV illustrates and analyses the experiments and results. Section V concludes the research work and future directions.

II. ROBOT CONFIGURATION AND MODELLING

The basic motion modes of the human ankle joint (Fig. 1) can be divided into three DOFs: dorsiflexion/ plantarflexion, inversion/ eversion, and internal rotation/ external rotation. Carl *et al*. pointed out that the former two DOFs play a major role in the ankle exercise and rehabilitation [21]. Based on the principle of ankle movement and its recovery requirements, this paper presents a 2-DOF soft ankle rehabilitation robot actuated by PMs in parallel configuration.

A. Ankle Robot Development

The whole system of the parallel PMs-actuated ankle rehabilitation robot is shown in Fig. 2, including the robot body, control module, communication module and host computer. Each PM (FESTO MAS-20-400N) is controlled by the corresponding pressure proportional valve (FESTO

VPPM-6L-G18-0L6H), while its output force and position are monitored by a force sensor (BSQ-2) and displacement sensor (MLO-POT-225-TLF). Through the A/D data acquisition card (NI USB-6210), these sensing signals are sent to the host computer, and then processed by the control system based on LabVIEW. After the conversion of the D/A data acquisition card (ZTIC USB-7660BD), the control signals are imported into proportional valve, thus controlling the PMs to actuate the movement of the robotic platform.
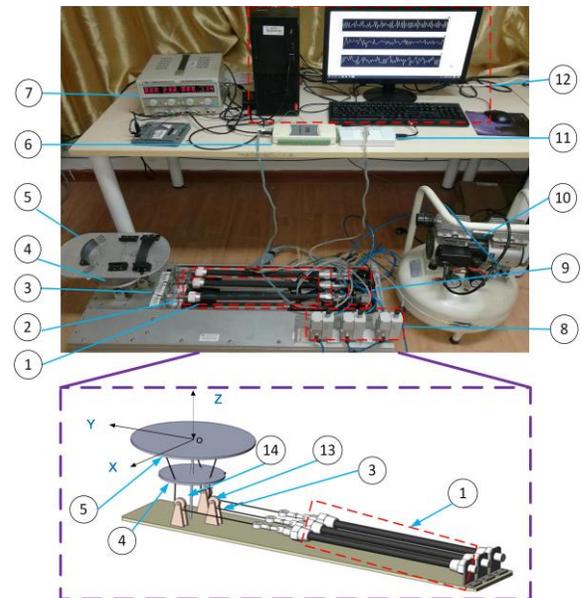

Fig.1. Model and motion DOFs of the ankle joint.

Fig.2. Configuration of the ankle rehabilitation robot. ① pneumatic muscle actuator, ② displacement sensor, ③ cable, ④ fixed platform, ⑤ moving platform, ⑥ D/A data acquisition card, ⑦ DC power, ⑧ pressure proportional regulator, ⑨ force sensor, ⑩ air pump, ⑪ A/D data acquisition card, ⑫ host computer, ⑬ pulley, ⑭ support stick.

The soft ankle rehabilitation robot is mainly composed of three PM actuators, a moving platform and a fixed platform, as shown in Fig.2. Since the PMs in the parallel configuration can only generate unidirectional pulling force, a redundant drive is necessarily introduced to enable all the cables connected between PMs and moving platform keeps in tension. Hence the 2-DOF parallel ankle rehabilitation robot is driven by three PMs. The parallel PMs connected the moving platform with cables through the pulleys and corresponding holes on the fixed platform. The moving platform and the fixed platform are connected by a vertically-placed rigid support stick. The lower end of the stick is secured at the fixed platform, while the upper one is connected with the moving platform through the Hooke's hinge, to ensure that the moving platform can only rotate around X axis and Y axis.

B. Kinematics Modelling

The geometrical model of the robot' parallel PMs-actuated configuration is presented in Fig.3. b_1, b_2 and b_3 are the connection points of the cables and the fixed platform, while B_1, B_2 and B_3 are the coordinate points of cables secured at the fixed platform. O' and O represent the connected points of the support stick and the moving/ fixed platform, respectively. The distance between O' and b_3, b_2, b_1 are $h_1 = 0.08$ m, $h_2 = 0.07$ m, while that of O and B_1, B_2, B_3 are $H_1 = 0.08$ m, $H_2 = 0.07$ m, and $O'O = 0.09$ m. The angle of α and β are $50°$ and $80°$, respectively.
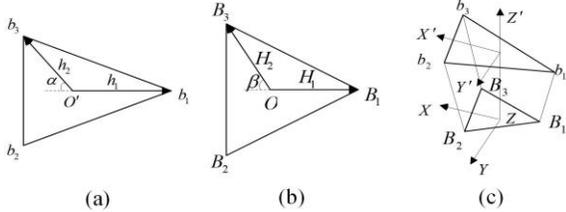

Fig.3. The geometrical model of the parallel PMs-actuated ankle robot. (a) and (b) are the geometrical parameters of the moving platform and fixed platform, (c) is the whole geometrical model.

The kinematic model describes the relationship between the robot's end effector posture and the displacement of the multiple PM actuators. Thus based on the kinematic model, we can control the length of the PMs synchronously to adjust robot's posture and enable the robot to follow the desired trajectory. As shown in Fig.3, $O' - X'Y'Z'$ and $O - XYZ$ are the established coordinate systems of the moving platform and the fixed platform, respectively. Assuming that the moving platform rotates θ around X axis and then rotates ϕ around Y axis, thus the robot's posture transformation matrix of the fixed coordinate system to the moving one is described as:

$$\begin{aligned} R &= R(y, \theta)R(x, \phi) \\ &= \begin{bmatrix} cos\phi & sin\phi sin\theta & sin\phi cos\theta \\ 0 & cos\theta & -cos\theta \\ -sin\phi & cos\phi cos\theta & cos\phi cos\theta \end{bmatrix}. \end{aligned} \tag{1}$$

The vectors of the moving/fixed platform's endpoints are respectively denoted as r_{b_i}' and r_{B_i} in their original coordinate systems, which can be expressed as:

$$r_b' = [r_{b_1}' \quad r_{b_2}' \quad r_{b_3}'] = \begin{bmatrix} -h_1 & h_2 cos\alpha & h_2 cos\alpha \\ 0 & h_2 sin\alpha & -h_2 sin\alpha \\ 0 & 0 & 0 \end{bmatrix}, \tag{2}$$

$$r_B = [r_{B_1} \quad r_{B_2} \quad r_{B_3}] = \begin{bmatrix} -H_1 & H_2 cos\beta & H_2 cos\beta \\ 0 & H_2 sin\beta & -H_2 sin\beta \\ 0 & 0 & 0 \end{bmatrix}. \tag{3}$$

Based on (1)-(3), it can be calculated that the vectors of cables from the endpoints of the fixed platform $O - XYZ$ to the corresponding ones in the coordinate system $O' - X'Y'Z'$, as presented in (4), where P is the vector between the fixed platform's origin O and O' of the moving one.

$$L = r_b' T + P - r_B, \tag{4}$$

Thus the length of the cables between the two platforms is:

$$l = \sqrt{L^T L}. \tag{5}$$

C. Dynamics Modelling

To achieve high-precision motion control of the robot driven by PMs, the robot's dynamic model plays an important role which can help us understand the force relationship of the cooperative PMs. Based on (1), the generalized coordinate of the moving platform can be defined as $q = [\theta, \phi, 0]^T$, and then the generalized velocity of the platform is:

$$\dot{q} = \omega = \widetilde{E}\begin{pmatrix} \dot\theta \\ \dot\phi \\ 0 \end{pmatrix} = \begin{bmatrix} cos\phi & 0 & 0 \\ 0 & 1 & 0 \\ -sin\phi & 0 & 1 \end{bmatrix}\begin{pmatrix} \dot\theta \\ \dot\phi \\ 0 \end{pmatrix}. \tag{6}$$

Thus the dynamic model of the robot can be established according to the Lagrange's equation, as expressed by:

$$M(q)\ddot{q} + C(q, \dot{q})\dot{q} + G(q) = F_l, \tag{7}$$

where $M(q)$, $C(q, \dot{q})$, $G(q)$ and F_l are the inertial matrix, Coriolis centrifugal force matrix and gravity matrix, output torque matrix of the robot respectively.

Based on (1) - (6), the parameters of (7) can be obtained:

$$\begin{cases} M(q) = TI_P T^T \\ C(q, \dot{q}) = \widetilde{\omega} TI_P T^T \\ G(q) = m\widetilde{T}_{r_m} \widetilde{\omega}^2 Tr_m \end{cases}, \tag{8}$$

where ω has been descripted in (6) that $\omega = \dot{q}$, and m is the mass matrix of the moving platform, I_P and r_m are the rotation inertia and the mass center of the moving platform in its coordinate system respectively, and $\widetilde{T}_{r_m}$ is the helix matrix of Tr_m.

III. COUPLING DISTURBANCE COMPENSATED MIMO SLIDING MODE CONTROLLER

The PMs in parallel configuration would cause coupling interference during the synchronous movement, especially when the human interacts with the robot. To address this problem, a coupling disturbance compensated MIMO sliding mode controller compensation is proposed.

A. MIMO Robotic System

Based on the dynamic model in (7)-(8), the multi-input-multi-output rehabilitation robot can be defined as:

$$\begin{cases} y_v = \dot{y} \\ \dot{y}_v = -M^{-1}(Cy_v + F_l - G) \end{cases}, \tag{9}$$

where $y = [y_1 \quad y_2 \quad y_3]$ and $\dot{y} = [\dot{y}_1 \quad \dot{y}_2 \quad \dot{y}_3]$ are the actual position vector and velocity vector of PMs.

To decrease the complexity of the dynamic model in (7) - (8) and control system of the parallel PMs-actuated robot, several unmodeled elements of the PM's characteristics are neglected. However, this may cause the modelling error in the PM's dynamic model, thus the disturbance estimation elements are introduced in the model. The total modelling disturbance can be expressed as:

$$\sigma_d = \widetilde{F}_l - \widetilde{B}\dot{y}_v - \widetilde{C}\dot{y} - \widetilde{G}\,, \tag{10}$$

where $\widetilde{F}_l$, $\widetilde{B}$, $\widetilde{C}$ and $\widetilde{G}$ are disturbance element of the inertial matrix, Coriolis centrifugal force matrix and gravity matrix, respectively. Additionally, during the robot-assisted ankle rehabilitation, the patient's foot also exerts force on the robotic platform, resulting in the interference during robot movement and deviation from the desired trajectory. And the PMs in parallel configuration amplify the interference error, which may cause the secondary injury to the patient. Thus the disturbance $\sigma_k(y)$ caused by the coupling interference can be expressed as a chaos movement [22] as in (10).

$$\begin{cases} \sigma_k(y) = \Lambda_{it}y + \Lambda_{cou}T_{cou}(y) \\ T_{cou}(y) = [y_2y_3 \quad y_1y_3 \quad y_1y_2] \end{cases}\,, \tag{11}$$

where $T_{cou}(y)$ is the element to describe the influence of other PMs on the targeted PM. Λ_{it} and Λ_{cou} are the coefficients for the coupling disturbance elements. Both of them are related to the ankle joint's interaction force exerted on the robotic platform. Thus (9) is rewritten as:

$$\begin{cases} \dot{y} = y_v \\ \dot{y}_v = -M^{-1}(C\dot{y} + F_l - G) - M^{-1}\sigma_d + \sigma_k(y) \end{cases}\,. \tag{12}$$

B. Coupling Disturbance Compensated Controller

For a sliding mode controller, the Lyapunov function can be defined as:

$$V = \frac{1}{2}s^Ts\,, \tag{13}$$

where s is the sliding surface. When the speed of the controlled object is close to zero, i.e., the controlled object is close to the sliding surface.

According to (12), the switch function can be defined as:

$$s = ky + \psi_{\sigma_d} + \psi_{\sigma_k}\,, \tag{14}$$

where k is a coefficient matrix related to the dynamic model. While ψ_{σ_d} and ψ_{σ_k} are disturbance compensation elements for modelling uncertainty and coupling interference in the parallel PMs-actuated robot, respectively.

Based on (10) and (14), ψ_{σ_d} can be defined as:

$$\begin{aligned} \psi_{\sigma_d} &= -kM^{-1}\sigma_d \\ &= -kM^{-1}(\widetilde{F}_l - \widetilde{B}\dot{y}_v - \widetilde{C}\dot{y} - \widetilde{G})\,. \end{aligned} \tag{15}$$

The coupling interference compensated element is defined:

$$\psi_{\sigma_k} = \tau_{pos}(\sigma_k(y), e, \dot{e}) + \tau_{force}(F_{int}) - \dot{\psi}_{\sigma_k}\,, \tag{16}$$

where e and $\dot{e}$ are the actual trajectory tracking error and speed error; F_{int} represents the ankle joint's force exerted on robotic platform. $\tau_{pos}(\sigma_k(y), e, \dot{e})$ is to compensate the interference from other two PMs, while $\tau_{force}(F_{int})$ is the forward compensation element for the disturbance caused by human-robot interaction force. (16) can effectively regulate the poles of the closed-loop control system, to reduce the coupling disturbance and avoid the singular posture.

According to (11), $\tau_{pos}(\sigma_k(y), e, \dot{e})$ in (16) is defined as:

$$\begin{aligned} \tau_{pos}(\sigma_k(y), e, \dot{e}) &= \sigma_k(y) + (\varepsilon_2 e + \varepsilon_3 \dot{e}) \\ &= \varepsilon_1(\Lambda_{it} \cdot y + \Lambda_{cou} \cdot T_{cou}(y)) + (\varepsilon_2 e + \varepsilon_3 \dot{e})\,, \end{aligned} \tag{17}$$

where $\varepsilon = [\varepsilon_1 \quad \varepsilon_2 \quad \varepsilon_3]$ is weight coefficient vector.

Since the influence of ankle's interaction force F_{int} on PMs in the robotic joint workspace is irregular and unpredicted, a F_{int} related higher-order polynomial is utilized to describe $\tau_{force}(F_{int})$ as:

$$\tau_{force}(F_{int}) = \kappa_1 F_{int} + \kappa_2 F_{int}^2 + \kappa_3 F_{int}^3, \tag{18}$$

where κ_1, κ_2 and κ_3 are experimental data-based coefficients.

According to (12) and (14),

$$\dot{s} = -kM^{-1}((C\dot{y} + F_l - G) + u) + \psi_{\sigma_d} + \dot{\psi}_{\sigma_k}. \tag{19}$$

Then from (13) we can obtain:

$$\dot{V} = s^T\dot{s} \tag{20}$$

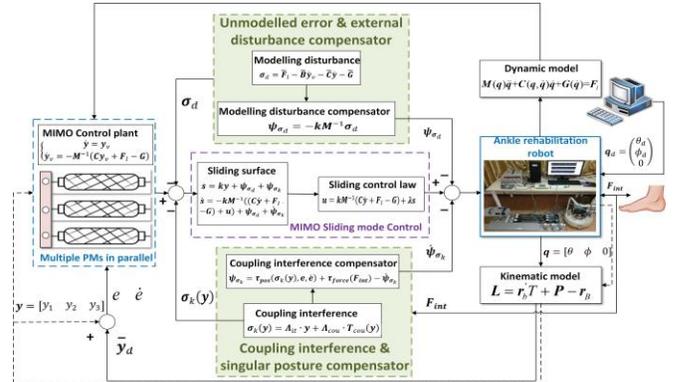
Fig.4. Block diagram of the proposed MIMO-DCSMC controller.

Substituting (19) into (20),

$$\begin{aligned} \dot{V} &= s^T(-kM^{-1}(C\dot{y} + F_l - G) + u) + \psi_{\sigma_d} + \dot{\psi}_{\sigma_k}) \\ &\leq s^T(-kM^{-1}(C\dot{y} + F_l - G) + u) + \psi_{\sigma_d} + \dot{\psi}_{\sigma_k} - \lambda s)\,, \end{aligned} \tag{21}$$

where the elements λ_{ij} in λ are all satisfied that $\lambda_{ij} > 0$.

Thus

$$\dot{V} \leq \lambda\|s\| \leq 0. \tag{22}$$

Then we can get that $\dot{V} \leq 0$ if the value of k are set as suitable values, and the system can be guaranteed stable. Thus the control law of the coupling disturbance compensated multi-input-multi-output controller (MIMO-DCSMC), as shown in Fig.4, can be expressed as:

$$u = kM^{-1}(C\dot{y} + F_l - G) - \psi_{\sigma_d} - \dot{\psi}_{\sigma_k} + \lambda s. \tag{23}$$

IV. EXPERIMENTAL RESULTS AND DISCUSSION

A. Response to Abrupt Posture Changes

When there is an obviously abrupt change in the robot's posture, the PMs in the parallel configuration will suddenly engage in a synchronized 'jumping' movement, which cause sharply increasing coupling interference for the PMs. To verify the control performance of the proposed MIMO-DCSMC strategy, a series of comparative trajectory

tracking experiments with the existing SMC were carried out on the actual ankle rehabilitation robot presented in Section II. We conducted a response experiment with posture abrupt changes of 10° around X-axis and Y-axis at the same time. The experimental results are shown in Fig.5.
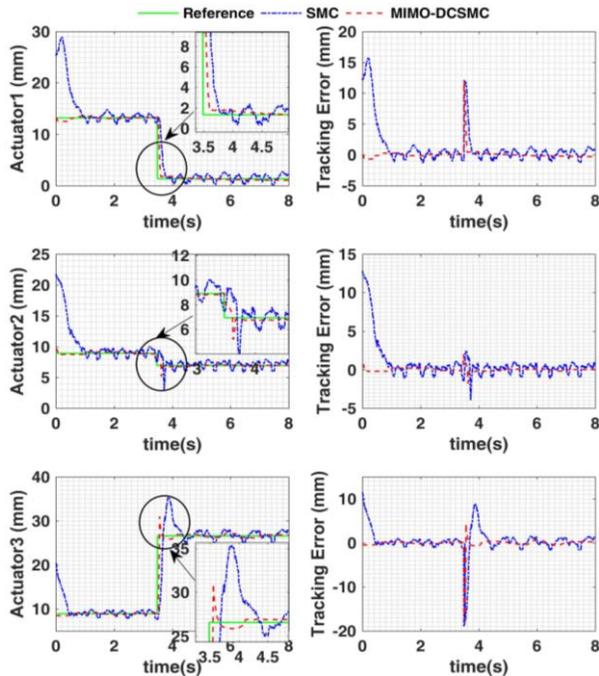

Fig.5. Response to abrupt posture change of the PMs-driven robot.

As shown in Fig.5, when the robot's posture changed suddenly, the proposed controller took 0.17s to address the coupling interference and enable the robot to reach the new desired trajectory, which is 80.46% faster compared with SMC. Additionally during the process, there was a serious overshoot problem in SMC scheme, especially for Actuator 3 with 8.75 mm, which is 48.69% of the whole motion range. The overshoot problem is not only caused by the PM's hysteresis characteristics, and other parallel PMs also produce external disturbance force at the PM when there is a sudden posture change. While the MIMO-DCSMC system can effectively reduce the overshooting problem by 49.6% compared with SMC. Thus MIMO-DCSMC performs high accuracy and better response performance for the parallel PMs-actuated robot during its abrupt change process.

B. Dynamic Trajectory Tracking

To further confirm the control performance for the ankle rehabilitation robot with patient's participation in clinic application conditions, the dynamic trajectory tracking experiments were carried out. The desired trajectory is a sinusoidal movement with frequency of 0.25 Hz and range of 10° around X-axis and Y-axis, respectively. The experiments were divided into two stages, and there three healthy subjects (one female and two males) were involved in Stage II. During the test, the subject placed his/her foot on the robot's moving platform, and the robot assist the subject's ankle to follow the desired trajectory. The PMs' experimental results of one subject are shown in Fig.6, while more detailed experimental data of all subjects are shown as TABLE I.
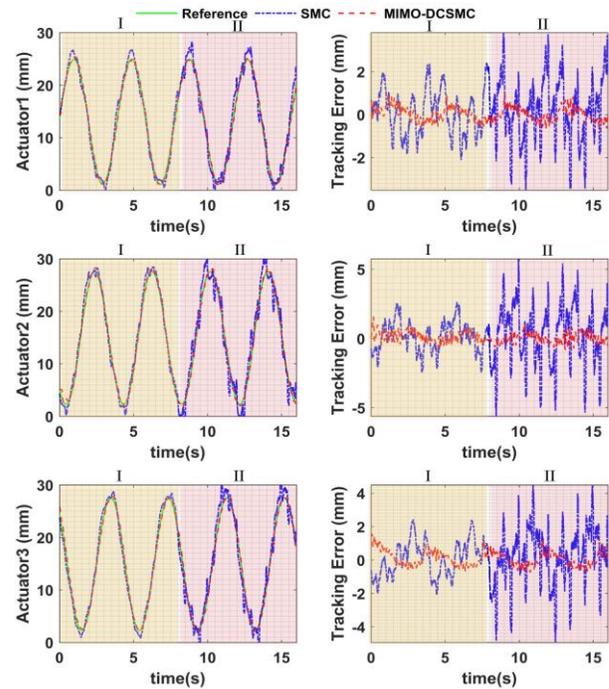

Fig.6. Sinusoidal trajectory tracking experiment of the ankle rehabilitation robot. Stage I has no subject, Stage II is conducted with one subject.

TABLE I   TRACJECTORY TRACKING RESULTS OF PMs

Stage	Actuators	SMC		MIMO-DCSMC	
		$AE^{\,a}$	$ME^{\,b}$	AE	ME
Stage I	Actuator1	0.800	2.526	0.274	0.962
	Actuator2	1.032	3.315	0.296	1.585
	Actuator3	0.876	2.800	0.368	1.561
Stage II	Actuator1	1.299	4.087	0.348	1.402
	Actuator2	1.846	5.785	0.360	1.908
	Actuator3	1.447	5.059	0.377	1.960

[a] ME= Max error (mm), [b] AE= Average Error (mm).

The average tracking error (AE) of SMC experienced an obvious increase by 69.54% with the subject, and its maximum tracking error (ME) reached 5.785 mm for Actuator 3.This also proves that the subject brings unpredictable and irregular disturbance to the high-precision control of the robot, which is hard to be included in the dynamic model. However, the human-robot interaction is an essential and inevitable issue in the robot-assisted rehabilitation system. Although the control performance of MIMO-DCSMC was weakened to some extent from Stage I to II, its ME is always smaller than 2 mm. This confirms that the proposed controller has an enhanced control capacity towards unmodeled and unpredictable disturbance, especially under the interaction with human subjects. Then, based on the PMs' actual displacement as shown in Fig.6, we obtained the trajectory of the robot's moving platform according to the robot forward kinematics, which is presented in Fig.7. In the absence of patient participation, both of SMC and MIMO-DCSMC could achieve relatively smooth trajectory tracking, but the performance the proposed controller presents higher precision increased by 28.57% compared with SMC (TABLE II). At Stage II, SMC could not effectively address the interference caused by the subject's interaction force, resulting in several sharp deviations of 6.14°, which is 30.7% of the whole motion

range. This is because the subject's foot inevitably causes the disturbance for the motion control of the robot itself, in addition the parallel configuration of the PM actuators will amplify the interference errors. The sharp disturbance may cause the secondary injury to patients in the actual rehabilitation. While the disturbance compensator of the controller is able to effectively tackle the modelling uncertainty and the coupling interference with subject's participation. Its maximum tracking error around X-axis and Y-axis were decreased by 42.05% and 54.89% compared with SMC. This proves that MIMO-DCSMC enable the parallel PMs-actuated ankle robot to provide the patients with safer and higher-precision motion assistance.
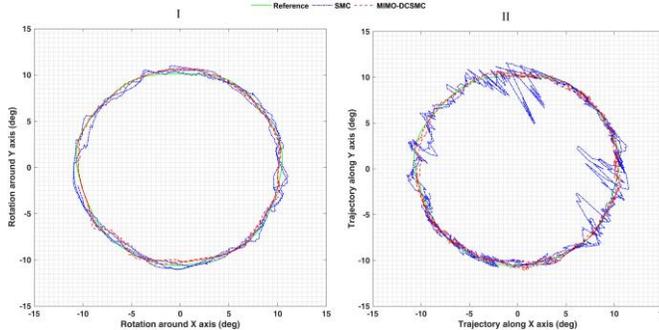

Fig.7. Tracking results of the ankle rehabilitation robot's moving platform. Stage I has no subject, Stage II is conducted with one subject.

TABLE II TRACJECTORY TRACKING RESULTS OF THE ANKLE REHABILITATION ROBOT'S MOVING PLATFORM

Stage	Movement	SMC		MIMO-DCSMC	
		AE^{a}	ME^{b}	AE	ME
Stage I	X-axis	0.55	2.63	0.35	1.74
	Y-axis	0.50	2.15	0.41	1.95
Stage II	X-axis	1.50	3.71	0.60	2.15
	Y-axis	1.45	6.14	0.45	2.77

[a] ME= Max error (deg), [b] AE= Average Error (deg).

V. CONCLUSION

This paper presents a novel soft ankle rehabilitation robot actuated by multiple pneumatic muscles in parallel, to provide compliant and sufficient assistance for the ankle joint rehabilitation. To tackle the modelling uncertainty caused by the PM's hysteresis and time-varying characteristics, as well as coupling interference in multiple parallel PMs, we proposed a coupling disturbance compensated MIMO sliding mode controller. A comparative experiment study between MIMO-DCSMC and SMC involving subject confirmed that the proposed controller is able to effectively enhance the robotic system's capability of tackling uncertainties and coupling interference in actual environment. With the MIMO-DCSMC, the ankle rehabilitation robot is able to provide the patient with suitable assistance to complete high-accuracy tracking tasks in rehabilitation. In this paper, the initial control parameters of MIMO-DCSMC were determined by trials and experiences. Further study will introduce adaptive regulation in the controller, to enable the control parameters adjusted in real-time according to the human-robot interaction.

REFERENCES

[1] http://www.cdc.gov/dhdsp/data_statistics/fact_sheets/fs_stroke/.
[2] W. Meng, Q. Liu, Z. D. Zhou, Q. S. Ai, and S. Q. Xie, "Recent development of mechanisms and control strategies for robot-assisted lower limb rehabilitation," *Mechatronics*, vol. 31, pp. 132-145, 2015.
[3] C. C. Hong, C. J. Pearce, M. S. Ballal, and J. D. Calder, "Management of sports injuries of the foot and ankle," *Bone & Joint Journal*, vol. 98-B, pp. 1299-1312, 2016.
[4] E. Y. Han, S. H. Im, B. R. Kim, M. J. Seo, and M. O. Kim, *Medicine*, vol. 95, pp. 50-68, 2016.
[5] Y. Park, B. Chen, Perez Arancibia, D. Young, L. Stirling, R. J. Wood, *et al.*, "Design and control of a bio-inspired soft wearable robotic device for ankle-foot rehabilitation," *Bioinspiration & Biomimetics*, v 9, 2014.
[6] G. S. Sawicki and D. P. Ferris, "A pneumatically powered knee-ankle-foot orthosis (KAFO) with myoelectric activation and inhibition," *Journal of Neuroengineering & Rehabilitation*, vol. 6, pp. 23-39, 2009.
[7] K. E. Gordon, G. S. Sawicki, and D. P. Ferris, "Mechanical performance of artificial pneumatic muscles to power an ankle-foot orthosis," *Journal of Biomechanics*, vol. 39, pp. 1832-1841, 2006.
[8] W. Meng, S. Q. Xie, Q. Liu, C. Z. Lu, and Q. S. Ai, "Robust Iterative Feedback Tuning Control of a Compliant Rehabilitation Robot for Repetitive Ankle Training," *IEEE/ASME Transactions on Mechatronics*, vol. 22, pp. 173-184, Feb 2017.
[9] M. Zhang, S. Q. Xie, X. Li, G. Zhu, M. Wei, X. Huang, *et al.*, "Adaptive Patient-Cooperative Control of a Compliant Ankle Rehabilitation Robot (CARR) with Enhanced Training Safety," *IEEE Transactions on Industrial Electronics*, vol. PP, pp. 1-1, 2018.
[10] P. K. Jamwal, S. Hussain, and S. Q. Xie, "Three-Stage Design Analysis and Multicriteria Optimization of a Parallel Ankle Rehabilitation Robot Using Genetic Algorithm," *IEEE Transactions On Automatic Control*, vol. 12, pp. 1433-1446, 2015.
[11] S. Ganguly, A. Garg, A. Pasricha, and S. K. Dwivedy, "Control of pneumatic artificial muscle system through experimental modelling," *Mechatronics*, vol. 22, pp. 1135-1147, 2012.
[12] V. Sakthivelu, S.-H. Chong, M. H. Tan, and M. M. Ghazaly, "Phenomenological Modeling and Classic Control of a Pneumatic Muscle Actuator System," *Int. J. Control. Autom*, vol. 9, pp. 301-312, 2016.
[13] H. P. H. Anh and K. K. Ahn, "Hybrid control of a pneumatic artificial muscle (PAM) robot arm using an inverse NARX fuzzy model," *Engineering Applications of Artificial Intelligence*, vol. 24, pp. 697-716, 2011.
[14] D. H. Zhang, X. G. Zhao, and J. D. Han, "Active Model-Based Control for Pneumatic Artificial Muscle," *IEEE Transactions on Industrial Electronics*, vol. 64, pp. 1686-1695, Feb 2017.
[15] J. Fan, J. Zhong, J. Zhao, and Y. Zhu, "BP neural network tuned PID controller for position tracking of a pneumatic artificial muscle," *Technology & Health Care*, vol. 2, pp. 231-248, 2015.
[16] K. Xing, J. Huang, Y. Wang, and J. Wu, "Tracking control of pneumatic artificial muscle actuators based on sliding mode and non-linear disturbance observer," *Control Theor. A*, vol. 4, pp. 2058-2070, 2010.
[17] Q. Liu, D. Liu, W. Meng, Z. Zhou, and Q. Ai, "Fuzzy sliding mode control of a multi-DOF parallel robot in rehabilitation environment," *International Journal of Humanoid Robotics*, vol. 11, 2014.
[18] T. Madani, B. Daachi, and K. Djouani, "Modular-Controller-Design-Based Fast Terminal Sliding Mode for Articulated Exoskeleton Systems," *IEEE Trans on Control System Tech*, vol. PP, pp. 1-8, 2017.
[19] J. Cao, S. Q. Xie, and R. Das, "MIMO sliding mode controller for gait exoskeleton driven by pneumatic muscles," *IEEE Transactions on Control Systems Technology*, vol. 9, pp. 44-53, 2017.
[20] R. Bertani, C. Melegari, M. C. D. Cola, A. Bramanti, P. Bramanti, and R. S. Calabrò, "Effects of robot-assisted upper limb rehabilitation in stroke patients: a systematic review with meta-analysis," *Neurological Sciences*, vol. 38, pp. 1-9, 2017.
[21] C. G. Mattacola and M. K. Dwyer, "Rehabilitation of the Ankle After Acute Sprain or Chronic Instability," *J Athl Train*, vol. 37, pp. 413-429, 2002.
[22] H. Wen, W. Xu, and M. Cong, "Kinematic Model and Analysis of an Actuation Redundant Parallel Robot With Higher Kinematic Pairs for Jaw Movement," *IEEE Trans on Indus Elec*, vol. 62, pp. 1590-1598, 2015.